Available online at www.sciencedirect.com

ScienceDirect

Procedia CIRP 124 (2024) 789–792

www.elsevier.com/locate/procedia

13th CIRP Conference on Photonic Technologies [LANE 2024], 15-19 September 2024, Fürth, Germany

Application of output constraints to a physics-informed hybrid model for the prediction of the threshold of deep-penetration laser welding

Michael Jarwitz[a]*, Andreas Michalowski[a]

University of Stuttgart, Institut fuer Strahlwerkzeuge (IFSW), Pfaffenwaldring 43, D-70569 Stuttgart, Germany

*Corresponding author. *E-mail address:* michael.jarwitz@ifsw.uni-stuttgart.de

Abstract

Physics-informed hybrid models, the combination of physics and machine learning, have already shown considerable benefits for quantitative predictions of process constraints, such as the threshold of deep-penetration laser welding. However, despite the improved prediction accuracy and extrapolation capability of such models, there can still be cases where the predictions of the model, including the confidence region, result in values that are not consistent with physical boundary conditions. Therefore, this paper presents the application of additional output constraints to a physics-informed hybrid model to further improve the compliance of the model with physics. Gaussian processes are used for the machine learning model and output warping is used to incorporate the output constraints directly into the model. The approach is demonstrated at the example of a hybrid model for the prediction of the threshold of deep-penetration laser welding.

Keywords: Physics-informed machine learning; hybrid model; Gaussian processes; output constraints; output warping

1. Introduction

The laser is already well established as a manufacturing tool in many serial production processes. Since the laser is a very versatile tool [1], it is also well suited for the use in highly versatile and efficient manufacturing systems [1,2] which are becoming more and more important, especially for small batch-size manufacturing [2-6]. The model-based prediction of process constraints is essential to find reliable process parameters with reasonable effort. The combination of physical models with machine learning (ML) in the form of physics-informed machine learning models [7-10] represents a promising solution for this task. Gaussian processes (GPs) possess some properties which make them a favorable choice for the use in the machine learning part of such a model. GPs are able to model quasi arbitrary functions, are probabilistic models, and they usually perform good in sparse data situations, which is beneficial when acquiring the training data is expensive, as can often be the case in laser processing.

Such a physics-informed hybrid model has already been successfully used to predict the threshold of deep-penetration laser welding [11]. Despite the advantages that result from using such a model, still cases can be observed where the model predictions, including the confidence region, also include values that are not consistent with physical boundary conditions (i.e., negative values for the threshold of deep-penetration laser welding in that case) [11].

Applying additional output constraints to the model is one approach that can be used to enforce that the model predictions are consistent with physical boundary conditions and therefore to further increase the accuracy of the model predictions. Output warping [12] is a method that can be applied for this task when Gaussian processes (GPs) are used for the models. This allows to incorporate the output constraints directly into the GP framework of the model and therefore to maintain all the beneficial properties of a GP model.

Therefore, this paper presents the application of output warping to constrain the outputs of a physics-informed hybrid model to further increase the consistency of the model with

10.1016/j.procir.2024.08.226

physical boundary conditions. The required adaptions to the model are shown and the approach is demonstrated at the example of a hybrid model for the prediction of the threshold of deep-penetration laser welding. The model results are discussed and compared to results of an existing hybrid model without output constraints.

2. Materials and Methods

Modelling of the threshold of deep-penetration laser welding is considered. The model is based on a physics-informed hybrid model $f_{HM} = f_{PM} + f_{DM}$, where ML is applied to model the deviations between a physical model f_{PM} and experimental results by a difference model f_{DM} using a GP model, as already applied in [11]. To extend this model, the approach of warped GPs [12] is applied to constrain the model outputs. In order to be able to apply output warping to the hybrid model, the model has to be adapted in such a way, that the outputs of f_{HM} are directly modelled by a GP. This can be achieved by directly integrating f_{PM} as the mean function into a GP model (i.e. $m(\boldsymbol{x}) = f_{PM}$), which is equivalent to modelling the differences to f_{PM} with a GP with a zero mean function ($m(\boldsymbol{x}) = 0$) [13]. Therefore, the physics-informed hybrid model with output constraint f_{CHM} is modelled by a GP whose prior for the mean function is the physics-based model

$$f_{PM} = \frac{\lambda_{th} \cdot (T_V - T_0)}{A} \cdot \frac{\pi^{3/2}}{4} \cdot \sqrt{\frac{Pe}{4} + 1.275} \tag{1}$$

for the threshold of deep-penetration laser welding. Eq. (1) describes the value of P/d at which the onset of deep-penetration laser welding occurs for the case of a circular beam with uniform intensity distribution (also known as “top-hat”), as given by eq. (11) in [14]. Here, d is the diameter of the laser beam on the work piece surface, P the laser power, A the absorptivity and λ_{th} the thermal conductivity of the material. T_0 is the ambient temperature (assumed to be 20 °C) and T_V the evaporation temperature of the material. $Pe = (d \cdot v)/\kappa$ is the Péclet number, with v the welding speed and $\kappa = \lambda_{\mathrm{th}}/(\rho \cdot c_p)$ the thermal diffusivity, where c_p is the specific heat capacity and ρ the density of the material.

A squared exponential kernel function

$$k(\boldsymbol{x}_m, \boldsymbol{x}_n) = \theta_{scale} \cdot \left(\exp\left[-\frac{1}{2} \cdot \sum_{i=1}^{j} \frac{(x_{m,i} - x_{n,i})^2}{\theta_{l,i}^2} \right] \right) \tag{2}$$

is used, where θ_{scale} is an output scale parameter, and $\boldsymbol{x}_m$ and $\boldsymbol{x}_n$ are two j-dimensional vectors, each containing a set of j input features for the GP model for one data point. Automatic relevance determination (ARD) is applied where separate length scale parameters $\theta_{l,i}$ are used for each of the j input features. Assuming a homoscedastic noise with variance σ_n^2 results in the covariance matrix $\boldsymbol{C}$ having elements [15]

$$C_{mn}(\boldsymbol{x}_m, \boldsymbol{x}_n) = k(\boldsymbol{x}_m, \boldsymbol{x}_n) + \sigma_n^2 \cdot \delta_{mn}, \tag{3}$$

where δ_{mn} is the Kronecker delta.

Output warping is applied to constrain the outputs of f_{CHM} to values that are consistent with physical boundary conditions, in this case to positive values. For this purpose, the natural logarithm is used for the warping function f_W and the targets in the observation space y_t are transformed through f_W to obtain the targets in the latent space

$$z_t = \ln(y_t). \tag{4}$$

For a new test point $\boldsymbol{x}_{N+1}$, the median of the prediction of f_{CHM} in the observation space is given by [12]

$$y_{med}(\boldsymbol{x}_{N+1}) = f_w^{-1}\big(\bar{z}(\boldsymbol{x}_{N+1})\big) = \exp\big(\bar{z}(\boldsymbol{x}_{N+1})\big), \tag{5}$$

where [13,15]

$$\bar{z}(\boldsymbol{x}_{N+1}) = m(\boldsymbol{x}_{N+1}) + \boldsymbol{k}^T \cdot \boldsymbol{C}^{-1} \cdot \big(\boldsymbol{z}_t - m(\boldsymbol{x}_{N+1})\big) \tag{6}$$

is the mean of the prediction of the warped GP in the latent space with $m(\boldsymbol{x}_{N+1}) = \ln(f_{PM})$. The vector $\boldsymbol{z}_t$ comprises the observed target values in the latent space at the input points $\boldsymbol{x}_n$ for the N data points used to train the model, and the vector $\boldsymbol{k}$ comprises the elements $k(\boldsymbol{x}_n, \boldsymbol{x}_{N+1})$ for $n = 1, \ldots, N$.

The bounds of the confidence region (± one standard deviation) in the observation space in which approximately 68 % of the predictions lie are given by [12]

$$y_{med\pm\sigma}(\boldsymbol{x}_{N+1}) = f_w^{-1}(\bar{z}(\boldsymbol{x}_{N+1}) \pm \sigma) = \exp(\bar{z}(\boldsymbol{x}_{N+1}) \pm \sigma), \tag{7}$$

where [15]

$$\sigma^2 = c - \boldsymbol{k}^T \cdot \boldsymbol{C}^{-1} \cdot \boldsymbol{k} \tag{8}$$

is the variance of the predictions of the warped GP in the latent space, and the scalar $c = k(\boldsymbol{x}_{N+1}, \boldsymbol{x}_{N+1}) + \sigma_n^2$.

The input features $x = (\lambda_{\mathrm{th}}, T_V, A, Pe, v, d, \rho)$ of f_{CHM} are standardized individually, i.e. scaled to result in a distribution with zero mean and unit variance for the training data. For the calculation of f_{PM} as the mean function of the GP, the respective input features are rescaled to the original physical values first.

The model hyperparameters θ_{scale}, $\theta_{l,i}$, and σ_n^2 are optimized for the training of the GP model, using the ‘Adam’ optimizer with a learning rate of 0.1, minimizing the negative log likelihood given the output of the GP model and the training data. Experimental data of the threshold of deep-penetration laser welding for 1 µm lasers with a top-hat intensity distribution available in literature [16-18] are used for the training and testing of the model. The data comprise a wide a range of materials and process parameters. The ranges of material properties and process parameters covered by the data are given in Table 1.

Table 1. Ranges of process parameters and material properties covered by the experimental data.

Property or parameter	range
λ_{Laser} in µm	1.03 – 1.064

d in µm	100 - 1680
P in W	75 - 15800
v in m/min	3 - 100
Pe	≈ 0.1 - 700
λ_{th} in W/(m·K)	14.8 - 401
ρ in kg/m³	2700 - 8960

3. Results

Only the case of extrapolation is considered in the following. The model was trained with all experimental data with d = 100 µm – 600 µm (resulting in 91 training data points) and predictions were made for the remaining experimental data with d = 1680 µm (resulting in 18 test data points).

The results of the hybrid model *without* output constraint [11] (f_{HM}) are shown in Fig. (1) by the green triangles. The error bars indicate the confidence region given by the standard deviation obtained from the corresponding GP model. It can be seen that the confidence regions of the predictions of f_{HM} include negative values for the threshold condition for deep-penetration laser welding in some cases, which is physically implausible. This is especially the case for predictions that are close to the physically plausible limit of the deep-penetration threshold (i.e., close to zero). It is worth noting that the black-box ML model (purple circles in Fig. 1) predicts the same value in all cases. This behavior is to be expected, since a GP model with a constant mean function as prior was used for the black-box ML model, and the GP model defaults to its prior in the case of extrapolation.

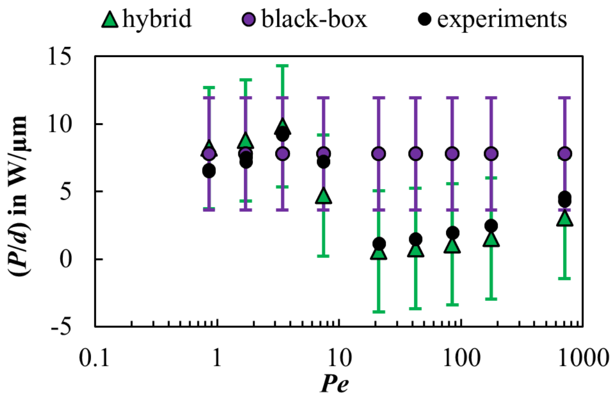

Fig. 1. Results of the hybrid model *without* output constraint, data from [11]. Black circles: experimental data; green triangles: results of the physics-informed hybrid model f_{HM}; purple circles: results of a black-box ML model f_{BB}. Error bars represent the standard deviation obtained from the respective GP model.

The results of the physics-informed hybrid model *with* output constraint (f_{CHM}) are shown in Fig. (2). The blue squares show the median of the predictions of f_{CHM} (given by eq. (5)) and the error bars indicate the confidence region of the model predictions, given by eq. (7). The predictions of f_{CHM} coincide with the results of the physics-based model f_{PM}, which is also to be expected, since the GP model defaults to f_{PM} as the prior for its mean function in this case. In contrast to f_{HM}, however, it can be seen that the confidence regions of the predictions of f_{CHM} only cover positive values, even for predictions close to the physically plausible limit of the deep-penetration threshold. This shows that the compliance of the model with physics could be further improved by applying the output constraint to the model. Furthermore, it can be seen that the confidence regions of the model predictions are asymmetric for f_{CHM}, which results from the mapping through the non-linear warping function f_W.

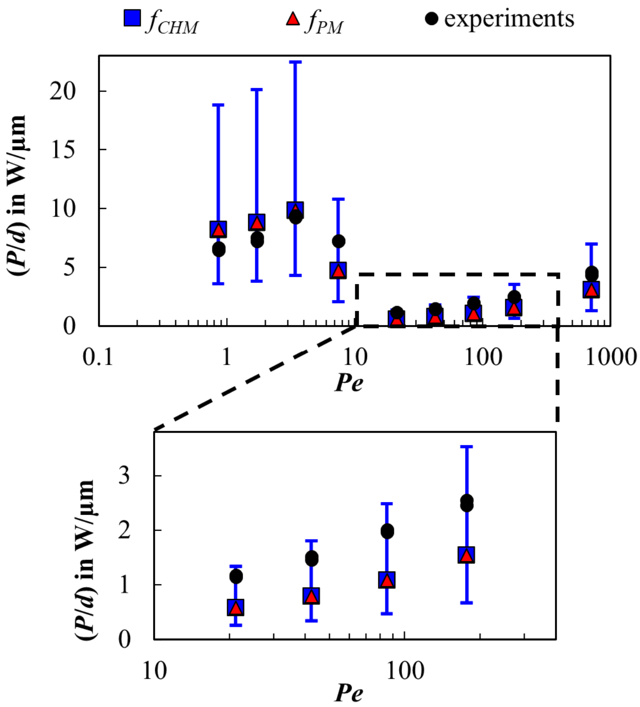

Fig. 2. Results of the hybrid model *with* output constraint. Black circles: experimental data; red triangles: results of the physics-based model f_{PM}; blue squares: results of the physics-informed hybrid model with output constraint f_{CHM}. Error bars indicate the confidence region given by the standard deviation obtained from the GP model.

4. Conclusion

In conclusion, we have demonstrated the application of output warping to constrain the outputs of a physics-informed hybrid model to further improve the compliance of the model with physics, limiting the model predictions, including the confidence interval, to physically plausible values.

Acknowledgements

The presented work was funded by the Ministry of Science, Research and the Arts of the Federal State of Baden-Wuerttemberg within the "InnovationCampus Future Mobility", which is gratefully acknowledged.

References

[1] Graf, T, Hoßfeld, M& Onuseit, V. A Universal Machine: Enabling Digital Manufacturing with Laser Technology. in ARENA2036, *Advances in Automotive Production Technology – Theory and Application*, P. Weißgraeber, F. Heieck, and C. Ackermann, Eds, Berlin, Heidelberg: Springer Berlin Heidelberg; 2021 p. 386–393

[2] Jarwitz, M, et al. Towards a universal manufacturing node: Requirements for a versatile, laser-based machine tool for highly adaptable manufacturing. Procedia CIRP 2022; 111 p. 816–821.

[3] Cohen, Y, et al. Design and management of digital manufacturing and assembly systems in the Industry 4.0 era. Int J Adv Manuf Technol 2019; 105:9 p. 3565–3577.

[4] ElMaraghy, H. Smart changeable manufacturing systems. Procedia Manufacturing 2019; 28 p. 3–9.

[5] Hu, SJ. Evolving Paradigms of Manufacturing: From Mass Production to Mass Customization and Personalization. Procedia CIRP 2013; 7 p. 3–8.

[6] Xu, L, et al. Reshaping the Landscape of the Future: Software-Defined Manufacturing. Computer 2021; 54:7 p. 27–36.

[7] Gauger, I, Nagel, T& Huber, M. Hybrides Maschinelles Lernen im Kontext der Produktion. in *Digitalisierung souverän gestalten II*, E. A. Hartmann, Ed, Berlin, Heidelberg: Springer Berlin Heidelberg; 2022 p. 64–79

[8] Karniadakis, GE, et al. Physics-informed machine learning. Nat Rev Phys 2021; 3:6 p. 422–440.

[9] Lee, J & Lai, A. Function-based and physics-based hybrid modular neural network for radio wave propagation modeling. in *IEEE Antennas and Propagation Society International Symposium. Transmitting Waves of Progress to the Next Millennium. 2000 Digest. Held in conjunction with: USNC/URSI National Radio Science Meeting (Cat. No.00CH37118)*: IEEE 2000 p. 446–449

[10] Psichogios, DC & Ungar, LH. A hybrid neural network - first principles approach to process modeling. AIChE Journal 1992; 38:10 p. 1499 - 1511.

[11] Jarwitz, M & Michalowski, A. Hybrid model for the threshold of deep-penetration laser welding. in *Proceedings of the Lasers in Manufacturing Conference (LiM)* 2023;

[12] Snelson, E, Ghahramani, Z& Rasmussen, C. Warped gaussian processes. Advances in neural information processing systems 2003; 16:.

[13] Rasmussen, CE & Williams, CKI. Gaussian processes for machine learning. 2nd ed. Cambridge, Mass.: MIT Press; 2006.

[14] Graf, T, et al. Analytical expressions for the threshold of deep-penetration laser welding. Laser Phys. Lett. 2015; 12:5 p. 56002.

[15] Bishop, CM. Pattern recognition and machine learning. New York: Springer; 2006.

[16] Fabbro, R. Melt pool and keyhole behaviour analysis for deep penetration laser welding. J. Phys. D: Appl. Phys. 2010; 43:44 p. 445501.

[17] Jarwitz, M. Laserstrahlschweißen von Metallen mit unterschiedlichen thermophysikalischen Eigenschaften.; 2020, Doctoral thesis, Institut fuer Strahlwerkzeuge, Universität Stuttgart, Stuttgart.

[18] Wagner, J. Ermittlung der Tiefschweißschwelle beim Laserstrahlschweißen von metallischen Werkstoffen.; 2015, Bachelor thesis, Institut fuer Strahlwerkzeuge, University of Stuttgart, Stuttgart.